Available online at www.sciencedirect.com
ScienceDirect
Trans. Nonferrous Met. Soc. China 31(2021) 3677−3690
Transactions of Nonferrous Metals Society of China
www.tnmsc.cn

Effect of NaOH on plasma electrolytic oxidation of A356 aluminium alloy in moderately concentrated aluminate electrolyte

Yu-lin CHENG[1], Huan-jun XIE[2], Jin-hui CAO[3], Ying-liang CHENG[1]

1. College of Materials Science and Engineering, Hunan University, Changsha 410082, China;
2. AECC Zhongchuan Transmission Machinery Co., Ltd., Changsha 410200, China;
3. College of Chemistry and Chemical Engineering, Hunan University, Changsha 410082, China

Received 22 November 2020; accepted 15 May 2021

Abstract: Plasma electrolytic oxidation (PEO) of cast A356 aluminum alloy was carried out in 32 g/L $NaAlO_2$ with the addition of different concentrations of NaOH. The stability of the aluminate solution is greatly enhanced by increasing the concentration of NaOH. However, corresponding changes in the PEO behaviour occur due to the increment of NaOH concentration. Thicker precursor coatings are required for the PEO treatment in a more concentrated NaOH electrolyte. The results show that the optimal NaOH concentration is 5 g/L, which improves the stability of storage electrolyte to about 35 days, and leads to dense coatings with high wear performance (wear rate: 4.1×10^{-7} $mm^3\cdot N^{-1}\cdot m^{-1}$).
Key words: plasma electrolytic oxidation; wear resistance; sodium aluminate; sodium hydroxide; A356 alloy

1 Introduction

Aluminium alloy has been widely used in the automotive and aerospace industries due to its significant advantages such as lightweight, high specific strength, and good machinability [1,2]. Besides, the introduction of silicon element could greatly increase the fluidity of Al [3,4], resulting in excellent castability of Al−Si alloys, such as A356 aluminum alloy [5,6]. However, there are still some bottleneck problems that limit the development of Al−Si alloys, such as low surface hardness, poor wear resistance and unsatisfactory corrosion resistance [7,8]. The surface performances of light metals, such as Al, Mg and their alloys, can be improved by a variety of surface treatment approaches, such as electroplating [9,10], chemical vapor deposition (CVD) [11], physical vapor deposition (PVD) [12], anodizing [13] and plasma electrolytic oxidation (PEO) [14−17]. Among these methods, PEO owns unique advantages, such as excellent corrosion, adhesion and ease of obtaining thick coatings.

PEO is an advanced surface treatment technique that evolves from the conventional anodic oxidation method and has been universally applicable to the so-called valve metals (Mg, Al, Zr, Ti, etc) and related alloys [18−24]. Unlike conventional anodizing, much higher voltages are needed for PEO to cause plasma sparks at the electrolyte/workpiece interface during the coating formation process [25]. PEO consists of various physical and chemical processes such as coating formation, dissolution, gas emission, dielectric breakdown and plasma generation, which bring challenges for researchers to understand and control the process [23,26]. For the PEO of Al and its alloys, it is known that the coatings undergo chemical dissolution and field-assisted dissolution [26,27], which are closely related to the alkaline concentration and applied current density,

Corresponding author: Ying-liang CHENG, Tel: +86-731-88821727, E-mail: chengyingliang@hnu.edu.cn, deepblacksea@163.com
DOI: 10.1016/S1003-6326(21)65756-4

respectively. Alkaline electrolytes are usually used in the PEO treatment, which is more eco-friendly than the acidic electrolytes used in conventional anodization. The most frequently-used PEO electrolytes are silicates, phosphates, tungstates and aluminates, which are the so-called inorganic polymers [28−30]. According to our previous work, coatings on Al−Cu−Li or Al−Si alloys prepared in the concentrated aluminate electrolyte exhibit excellent corrosion resistance and wear resistance [18,31]. However, the instability of the electrolyte, especially when the aluminate concentration is high, becomes a worrisome issue [31]. Thus, how to develop stable aluminate electrolytes with the capability to produce high-quality coatings becomes a challenge in PEO study.

According to the literature, the stability of aluminate solutions is related to the ratio of Na_2O to Al_2O_3, and the low molar ratio of Na_2O to Al_2O_3 is detrimental to the stability of the solution [32]. Hence, the addition of NaOH to the aluminate electrolyte may be a feasible way to make the electrolyte more durable. However, an improved NaOH concentration may affect the PEO process. MOON and JEONG [33] found that micro discharges on Al cannot be established when the concentration of NaOH is high. Hence, a detailed study of the PEO of Al alloys in aluminate electrolytes with enhanced NaOH concentration is necessary. In this work, NaOH (0−10 g/L) is added to enhance the stability of the concentrated aluminate electrolytes as well as to promote the formation of PEO coatings on A356 aluminium−silicon alloy workpiece. The stability of aluminate electrolyte with the addition of different concentrations of NaOH is investigated. Then, PEO behaviors and tribological properties of the coatings formed in electrolytes with different NaOH concentrations are investigated.

2 Experimental

Cast A356 aluminium alloy (Composition in wt.%: Si 7.014, Mg 0.293, Sr 0.011, Ti 0.128, Zn 0.005, Fe 0.108, Cu 0.002, Mn 0.002, Cr 0.002, Ni 0.004, Pb 0.001, Ca 0.001, Sn 0.001, and balance Al) was cut into small specimens, with one side connected with a copper wire for electric contact. After that, the specimens were mounted in epoxy resin to provide a working area of 10 mm × 20 mm. The exposed area was then polished down to 2000# SiC sandpaper, followed by alcohol degreasing, distilled water rinsing, and hot air drying. After that, the prepared specimen was assembled in a PEO setup as the anode, while a stainless steel plate served as the cathode. A 5 kW pulsed power source (MAO-5D, Pulsetech Electrical Co., Ltd., Chengdu, China) was used, and a water cooling system with magnetic stirring was employed to cool the electrolyte temperature below 40 °C. Pulsed bipolar constant current regimes with a frequency of 1000 Hz and a duty cycle of 20% were employed for the PEO treatment. An oscilloscope (Tektronix TDS 1002C-SC) was used to monitor the current waveforms, and the average positive and negative current densities determined from the waveforms were about 0.108 and 0.056 A/cm^2, respectively.

The electrolytes were 2 g/L $NaAlO_2$ + 1 g/L NaOH and 32 g/L $NaAlO_2$ with the addition of 1, 5 and 10 g/L NaOH, respectively. The electrolytes were prepared from high purity reagents (Sinopharm Chemical Reagent Co., Ltd, Shanghai, China) and distilled water. The stability of the aluminate electrolytes with different concentrations of NaOH was investigated by direct observation of the status of the electrolyte stored at a constant temperature of 25 °C with a water bath. Electrolyte conductivity was measured using a DDS-11A laboratory conductivity meter. The values of conductivity/resistivity of different electrolytes used in this study are listed in Table 1. The conductivity is improved as the concentration of $NaAlO_2$ and NaOH increases.

Table 1 Values of conductivity, resistivity (ρ) and lg ρ of PEO electrolytes used in this study (recorded at 20 °C)

Electrolyte	Conductivity/ ($S\cdot m^{-1}$)	Resistivity, ρ/($\Omega\cdot$m)	lg[ρ/($\Omega\cdot$m)]
2 g/L $NaAlO_2$ + 1 g/L NaOH	0.65	1.54	0.19
32 g/L $NaAlO_2$ + 1 g/L NaOH	2.88	0.35	−0.46
32 g/L $NaAlO_2$ + 5 g/L NaOH	3.68	0.27	−0.57
32 g/L $NaAlO_2$ + 10 g/L NaOH	4.76	0.21	−0.68

Although plasma discharges cannot be established directly on Al by PEO in NaOH electrolytes with high pH [33], we found that Al

alloys with a precursor coating can be treated in the high pH concentrated aluminate electrolyte, which was attributed to the inhibition of the chemical dissolution or field-assisted dissolution by the precursor coating [27]. However, in this work, it is found that thicker precursor coatings are needed for the PEO treatment in the electrolyte with a higher concentration of NaOH. The precursor coatings were obtained by treating the A356 alloy in 2 g/L $NaAlO_2$ + 1 g/L NaOH electrolyte for durations of 120−600 s in this study. After that, the A356 specimens were PEO-treated in 32 g/L $NaAlO_2$ electrolytes with the addition of 1, 5 and 10 g/L NaOH, respectively.

The surface and cross-sections of coatings were examined by scanning electron microscopy (SEM, QUANTA 2000 or Nova NanoSEM 230) and analyzed by energy-dispersive X-ray spectroscopy (EDS). Wear performance of the resultant coatings was tested by a CETR UMT-3 tribometer under dry sliding conditions (reciprocating motion, stroke length of 5 mm, frequency of 5 Hz, load of 20 N, WC (tungsten carbide) ball and sliding time of 1800 s). The WC ball has a diameter of 9.525 mm and a hardness value of HRA 91. Micro-hardness tests were made on A356 alloy substrate and the cross section of coatings, using the HX-1000TM/LCD digital microhardness tester with load of 25 g and dwell time of 10 s.

3 Results and discussion

3.1 Effect of aluminate concentration on micro-structure of coatings

Figure 1 presents the cross-sectional morphology of the obtained coatings after PEO treatment in 2 g/L $NaAlO_2$ + 1 g/L NaOH for 1200 s and 32 g/L $NaAlO_2$ + 1 g/L NaOH for 300 s, respectively. Precursor coating formed for 120 s was used when the alloy was treated in the concentrated electrolyte. It is obvious that the concentration of the electrolyte strongly affects the microstructure of the resultant coatings. Double-layered and single-layered coatings are formed in the electrolytes with low and high $NaAlO_2$ concentrations, respectively. The same regularity has been found in our previous studies when the influence of the electrolyte concentration on the coating microstructure is considered [34]. The single-layered coating is found to be more wear-resistant, compared with the double-layered counterparts [18]. However, the stability of the concentrated electrolyte of 32 g/L $NaAlO_2$ is poor, which greatly hinders the applicability of concentrated $NaAlO_2$ electrolyte in PEO [35−37].

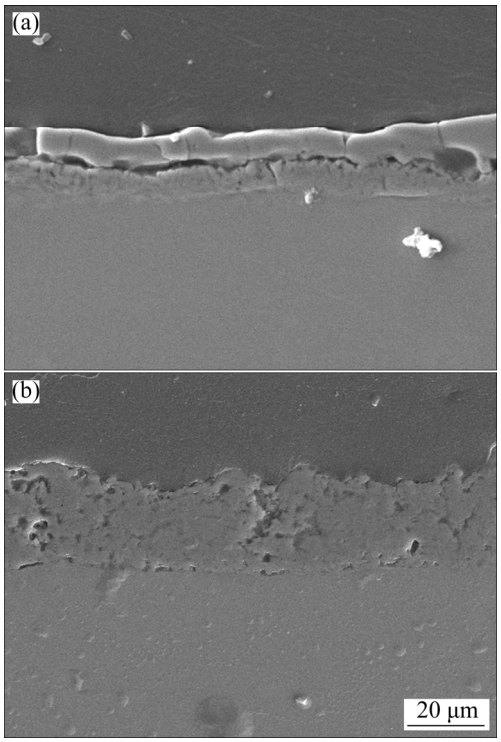

Fig. 1 SEM images showing cross sections of coatings formed in dilute and concentrated aluminate electrolytes: (a) 2 g/L $NaAlO_2$ + 1 g/L NaOH, 1200 s; (b) 32 g/L $NaAlO_2$ + 1 g/L NaOH, 300 s

3.2 Effect of NaOH on stability of $NaAlO_2$

The instability of the concentrated aluminate electrolytes may be caused by a series of reasons. Depending on the electrolyte concentration, preparation method, retention time and pH, the aluminate ion may have different structures, such as $Al(OH)_4^-$, $Al_2O(OH)_6^{2-}$, and $Al(OH)_6^{3-}$ [31,35,38−41]. As a result of the hydrolysis reaction of AlO_2^- ions, the tetrahedral of $Al(OH)_4^-$ ions is the main form of the aluminate species in solutions [27]:

$$AlO_2^- + 2H_2O = Al(OH)_4^- \quad (1)$$

However, the hydrolyzed $Al(OH)_4^-$ ions are easy to decompose into $Al(OH)_3$ in an aqueous solution according to Eq. (2) [42]:

$$Al(OH)_4^- = Al(OH)_3\downarrow + OH^- \quad (2)$$

The precipitation of $Al(OH)_3$ will be also promoted when CO_2 in the air enters the sodium

aluminate solution. The associated reaction is expressed by Eq. (3) [42]:

$$2Al(OH)_4^- + CO_2 = 2Al(OH)_3\downarrow + CO_3^{2-} + H_2O \quad (3)$$

However, it has been known that the stability of the $NaAlO_2$ electrolyte can be enhanced as the molar ratio of Na_2O to Al_2O_3 is increased [43] or simply by increasing the concentration of OH^- [37,44]. One reason may result from the fact that the CO_2 from the air can be consumed by Eq. (4):

$$NaOH + CO_2 = NaHCO_3 \quad (4)$$

As the pH of the solution is above 12, $NaHCO_3$ will be further converted into Na_2CO_3 according to Eq. (5):

$$NaHCO_3 + NaOH = Na_2CO_3 + H_2O \quad (5)$$

Hence, the detrimental effect of Eq. (3) is inhibited and the stability of the electrolyte is improved. Besides, adding more NaOH will facilitate the reverse reaction of Eq. (2), which suppresses the decomposition of the electrolyte.

In this work, different concentrations of NaOH (1, 5, 10 g/L) were added into 32 g/L $NaAlO_2$ electrolyte, and the stability of electrolyte was judged from the time for the occurrence of obvious precipitation. Figure 2(a) shows the appearance of the electrolyte containing 1 g/L NaOH after three days. White precipitates of $Al(OH)_3$ are present at the bottom of the bottle, indicating that the electrolyte is decomposed. However, the electrolytes with higher NaOH concentrations remain clear at this stage. After 35 days, an electrolyte containing 5 g/L NaOH begins to precipitate, but the electrolytes with 10 g/L NaOH is still stable (see Fig. 2(b)). It has been turned out that the electrolyte of 32 g/L $NaAlO_2$ + 10 g/L NaOH has been stored for more than 40 days without any sign of decomposition. Table 2 lists the time of stability for the concentrated aluminate electrolyte with different concentrations of NaOH. The observation of the stability of the electrolytes indicates that adding an appropriate concentration of NaOH is a feasible way to increase the stability of $NaAlO_2$ electrolyte.

3.3 Precursor coatings

It is well known that Al is an amphoteric metal, which means that the metal is unstable in both acidic and alkaline media. The surfaces of Al and its alloys are covered by a layer of original Al-related oxides. This oxide layer is stable in neutral pH. However, in alkaline solutions, it shows strong reactivity and typical reactions occur [33,45,46]:

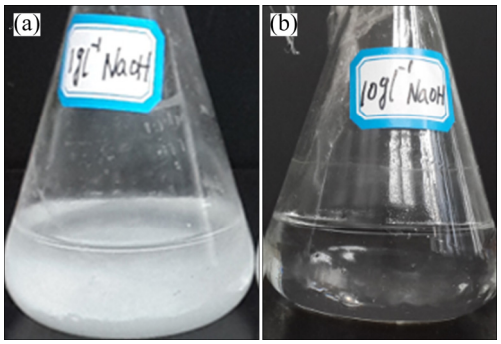

Fig. 2 Appearances of 32 g/L $NaAlO_2$ +1 g/L NaOH after 3 days (a), and 32 g/L $NaAlO_2$ +10 g/L NaOH after 35 days (b)

Table 2 Stability of 32 g/L $NaAlO_2$ with addition of different concentrations of NaOH as indicated by time with obvious precipitates appearing in electrolyte

NaOH concentration/(g·L^{-1})	1	5	10
Time of stability/d	1	35	>40

$$Al_2O_3 + OH^- = 2AlO_2^- + H^+ \quad (6)$$

$$AlOOH + OH^- = AlO_2^- + H_2O \quad (7)$$

$$Al(OH)_3 + OH^- = Al(OH)_4^- \quad (8)$$

The chemical dissolution of the original oxide on Al, represented by the above equations, is one of the reasons preventing the occurrence of plasma discharges and coating formation in higher concentration NaOH solutions [33]. Besides the chemical attack from the OH^-, the dissolution of the oxide film under the assistance of electric field, the so-called “field assisted dissolution”, is believed to contribute more to the dissolution of oxide films in concentrated aluminate with higher pH [27,47]. To overcome the problem of dissolution of original oxide film on Al and its alloys, thus ensuring a successful PEO coating formation process, precursor coatings were adopted when the Al alloy is treated in concentrated aluminate electrolytes [27]. The precursor coatings were usually fabricated by PEO of the alloy in a dilute electrolyte, e.g. 2 g/L $NaAlO_2$ + 1 g/L NaOH, for a short time of 60−120 s [27]. Figure 3 shows the typical SEM morphology of a precursor coating

formed on A356 alloy following PEO treatment in 2 g/L $NaAlO_2$ + 10 g/L NaOH for 120 s. A network of slightly protruding oxide materials is observed, which is due to the preferential oxidation of Al−Si eutectics distributed at the grain boundaries of A356 alloy [18]. Due to the short treatment time, the precursor coating only has a thickness of 1−2 μm. During PEO, the precursor coating is consumed or rebuilt to form the single-layered coating in concentrated aluminate electrolyte.

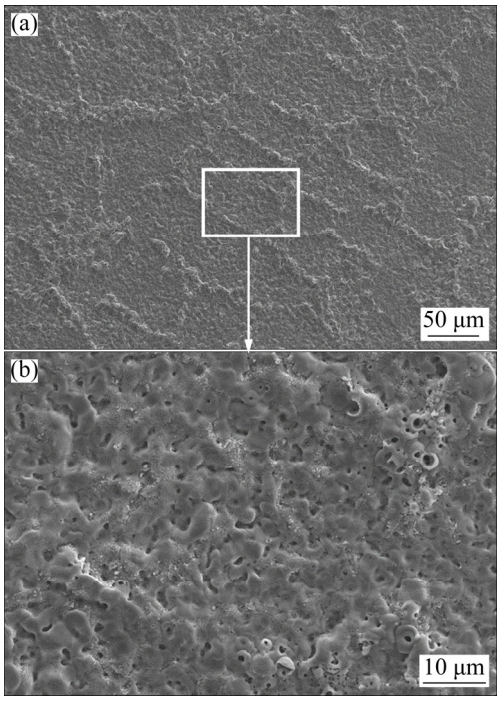

Fig. 3 SEM images of precursor coating formed by PEO treatment in 2 g/L $NaAlO_2$ + 10 g/L NaOH for 120 s

In this study, higher concentrations of NaOH are added in 32 g/L $NaAlO_2$ to keep the stability of the electrolyte. Hence, the electrolyte is more corrosive as the concentration of NaOH is enhanced. As a result, thicker precursor coatings are required for the PEO treatment in the electrolytes with higher NaOH concentrations.

3.4 PEO of A356 alloy in 32 g/L $NaAlO_2$ with addition of 1−5 g/L NaOH

Figure 4(a) shows the cell potential−time responses during the PEO of A356 alloy in electrolytes of 2 g/L $NaAlO_2$ + 1 g/L NaOH and 32 g/L $NaAlO_2$ with the addition of 1 and 5 g/L NaOH, respectively. Precursor coatings formed for 120 s are employed before the PEO of the alloy in the concentrated aluminates. The cell potentials are

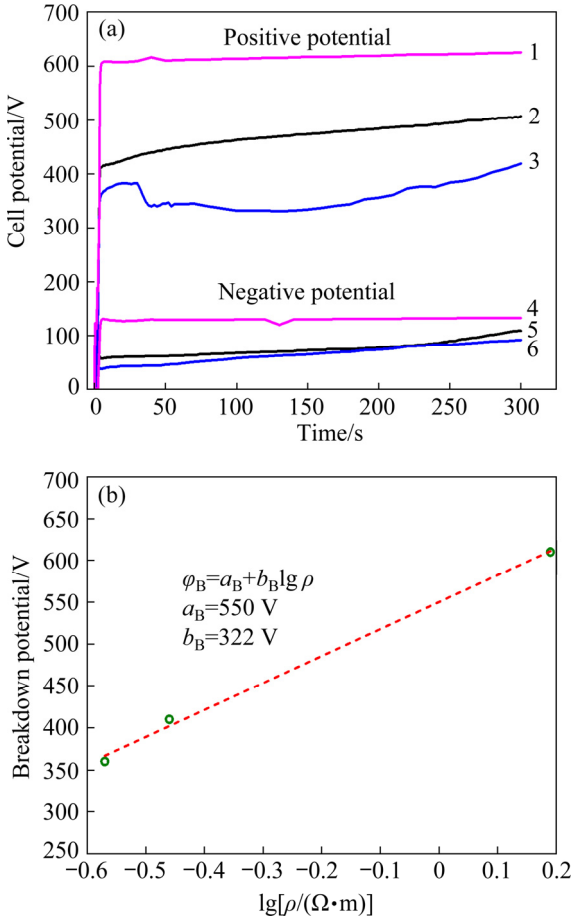

Fig. 4 Cell potential−time responses during pulsed bipolar PEO of A356 alloy in mixed electrolytes of aluminate and sodium hydroxide (1, 4 − 2 g/L $NaAlO_2$ + 1 g/L NaOH; 2, 5 – 32 g/L $NaAlO_2$ + 1 g/L NaOH; 3, 6 − 32 g/L $NaAlO_2$ +5 g/L NaOH) (a) and relationship between breakdown potential and lg ρ for PEO of alloy in three electrolytes (b) (Precursor coatings formed for 120 s were applied in more concentrated aluminate electrolytes)

peak values of the pulsed waveforms. For the PEO in the dilute electrolyte of 2 g/L $NaAlO_2$ + 1 g/L NaOH, the positive potential increases rapidly at the initial stage. When it reaches an inflection point after 4 s, plasma sparking occurs at the interface of electrolyte/workpiece, and thus the coating simultaneously begins to generate [48−50]. The inflection point is usually designated as the breakdown potential in literature [51]. The negative potential shows similar behavior to the positive one, but with much reduced values of about −130 V. Similar behaviors of positive and negative potentials are recorded for the PEO of the alloy in the concentrated electrolytes. However, lower values of breakdown potential are recorded

compared with those in the dilute electrolyte. IKONOPISOV [52] pointed out that the breakdown voltage is closely related to the type of anode metal, the electrolyte composition, and the resistivity of the electrolyte. Equation (9) is an empirical formula for calculating the breakdown potential (φ_B):

$$\varphi_B=a_B+b_B\lg\rho \quad (9)$$

where a_B and b_B are related to the anode metal and the composition of the electrolyte.

Equation (9) explains the phenomenon observed in Fig. 4(a). As the concentration of the electrolyte increases, the resistivity of the solution decreases, giving rise to a lower breakdown potential. Figure 4(b) plots the breakdown potential versus the logarithm of the electrolyte resistivity for the three electrolytes. The result agrees well with Eq. (9), revealing a_B and b_B values of 550 and 322 V, respectively. Owing to the lowered cell potential, the energy consumption of the PEO process was also reduced. Hence, the employment of a concentrated aluminate is beneficial from the point of view of energy saving.

Figure 5 shows cross-sectional morphologies of the coatings generated in 32 g/L $NaAlO_2$ + 1 g/L NaOH and 32 g/L $NaAlO_2$ + 5 g/L NaOH for 300 s. It is evident that both coatings are single-layered. The thickness values of the coatings formed in the aluminate electrolyte with the addition of 1 and 5 g/L NaOH are about 28 and 31 μm, respectively, which are averaged from eight different locations on the SEM cross sections. Furthermore, there seem to be fewer pores in Fig. 5(b), indicating that electrolyte of 32 g/L $NaAlO_2$ + 5 g/L NaOH might be of higher quality. It is pointed out that adding 5 g/L NaOH to the concentrated electrolyte not only improves the durability of the electrolyte but also results in coatings without altering its single-layered structure. One more point is that a precursor coating formed in the dilute aluminate electrolyte for 120 s is sufficient to ensure the establishment of plasma discharges and coating formation.

The microhardness of the two coatings shown in Fig. 5 has also been tested. Hardness values are based on ten test points on the cross sections. The coating formed in 32 g/L + 1 g/L NaOH shows an average hardness value of HV (908±65); however, a higher hardness value of HV (1188±60) is detected for the coating formed in 32 g/L + 5 g/L NaOH. Both values are significantly higher than the hardness of A356 substrate, which is about HV 115. The higher hardness of the coating formed in 32 g/L $NaAlO_2$ + 5 g/L NaOH may be attributed to the fact that it is denser in microstructure.

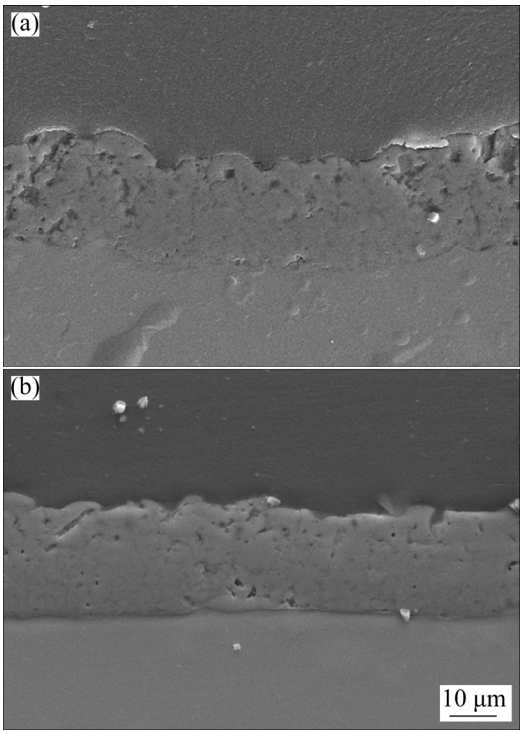

Fig. 5 SEM images showing cross sections of coatings formed for 300 s in 32 g/L $NaAlO_2$ + 1 g/L NaOH (a) and 32 g/L $NaAlO_2$ + 5 g/L NaOH (b) (Precursor coatings formed for 120 s were employed before the PEO)

3.5 PEO in 32 g/L $NaAlO_2$ + 10 g/L NaOH

Although a higher concentration of NaOH is better for the stability of the aluminate electrolyte, PEO cannot be easily carried out due to the improved corrosiveness of the electrolyte. A precursor coating formed for 120 s can be used in the concentrated aluminate electrolytes with 1−5 g/L NaOH; however, pretreatment of the A356 alloy in dilute electrolyte for 120 s cannot guarantee a successful PEO process in the electrolyte with the addition of 10 g/L NaOH. As a result, the alloy must be treated in the dilute electrolyte for a much longer time before it is then transferred into the concentrated electrolyte. This is actually a two-step PEO method. Figure 6 describes the cell potential–time responses of the PEO of A356 alloy in 32 g/L $NaAlO_2$ + 10 g/L NaOH, with precursor coatings formed for 120, 600 and 1200 s, respectively. Figure 6 shows that the positive potential of the

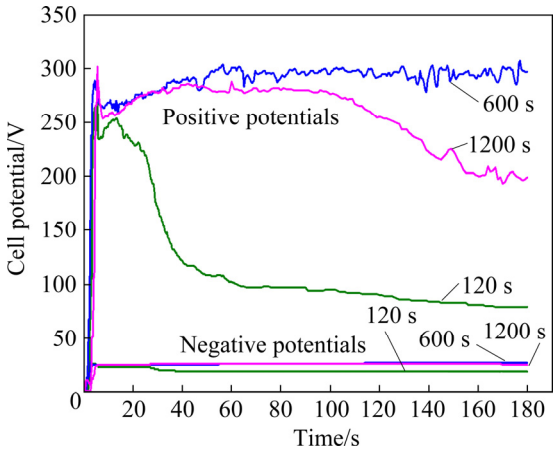

Fig. 6 Cell potential–time responses for PEO of A356 alloy in 32 g/L $NaAlO_2$ + 10 g/L NaOH with precursor coatings formed for 120, 600 and 1200 s, respectively, in dilute aluminate electrolyte

A356 alloy with the 120 s precursor coating drops rapidly after the initial rise, and then the potential is kept at low values less than 100 V after about 40 s. For the PEO of the alloy with precursor coating formed for 600 s, the positive potential does not drop during the whole PEO process for 180 s, with a final positive potential of about 300 V. A long pre-treatment time of 1200 s has been employed to form precursor coating on the A356 alloy and the PEO of the alloy with this precursor coating has also been carried out. In contrast to the PEO with the 600 s precursor coating, the positive potential begins to decline at about 50 s, reaching a final potential of about 200 V at 180 s. The result may indicate a longer preformed coating does not ensure a high positive potential during the PEO in the electrolyte with concentrated NaOH.

Figure 7 shows the surface morphologies of the A356 alloy after being PEO-treated in 32 g/L $NaAlO_2$ + 10 g/L NaOH for 180 s using the 120 s precursor coating. Cell potential curves in Fig. 6 indicate that the positive potential of this sample drops below 100 V at the later stage of PEO. Plasma discharges also vanish as the potential drops. The SEM image shows that the precursor coating still covers most areas of the alloy surface. However, a big pit with a size up to 100 μm is presented at the center of the image. Similar pits can also be found elsewhere on the alloy surface. The appearance of pits indicates that the precursor coating is damaged locally during the PEO in the concentrated electrolyte. The enlarged images of Figs. 7(b, c) clearly show that the exposed substrate under the pit has been corroded. High magnification image of Fig. 7(d), corresponding to the boxed region in Fig. 7(c), shows nano-sized pores with a

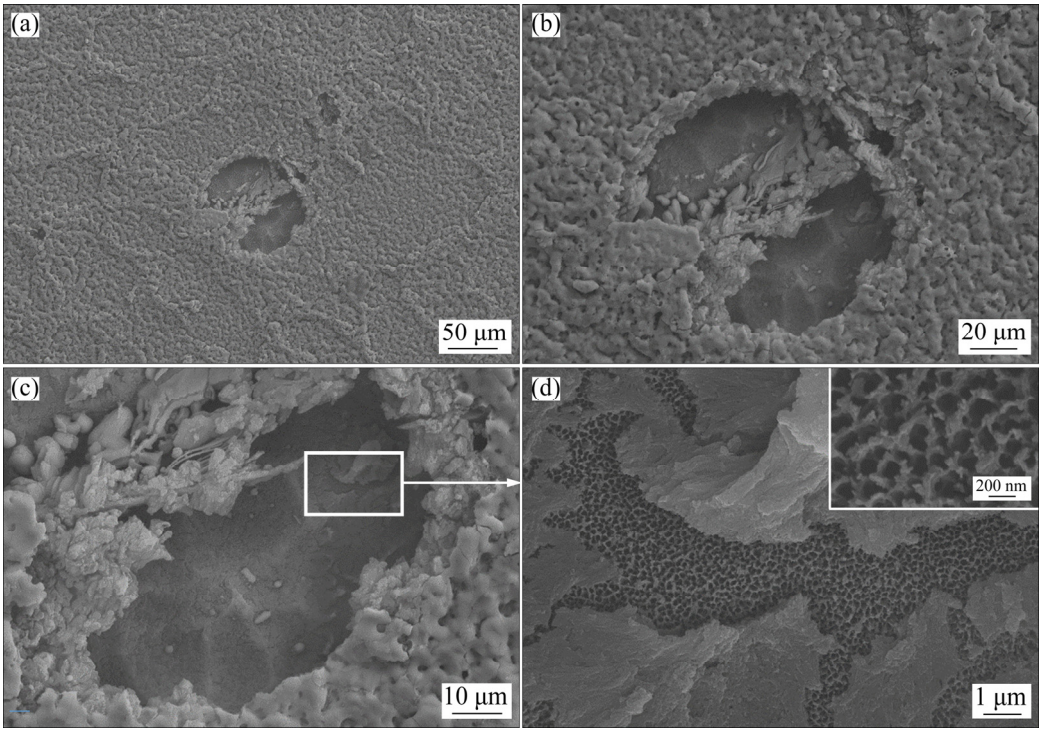

Fig. 7 SEM images showing surface morphologies of A356 alloy after being treated in 2 g/L $NaAlO_2$ + 1 g/L NaOH for 120 s to form precursor coating and then PEO-treated in 32 g/L $NaAlO_2$ + 10 g/L NaOH for 180 s

dimension of 100−200 nm. The formation of these pores may be due to the mechanism of conventional anodization. For example, YANG et al [53] observed a similar porous surface after PEO treatment of Al in $Na_5P_3O_{10}$ solution with the addition of 2 g/L NaOH. Compared with Fig. 3(b), it can be found that the precursor coating is destroyed (Fig. 7(b)).

Figures 8(a, c) present the cross-sectional images of the precursor coatings generated in 2 g/L $NaAlO_2$ + 1 g/L NaOH for 600 and 1200 s, respectively. These coatings show a bi-layered feature, which is consistent with our previous experience with the PEO in dilute electrolytes [34]. After the treatment of these bi-layered coatings in 32 g/L $NaAlO_2$ + 10 g/L NaOH for 180 s, the corresponding cross-sectional SEM images are shown in Figs. 8(b, d), respectively. Figure 8(b) shows that the precursor coating formed for 600 s has been converted into the single-layer structure; however, a great number of fine pores are presented in the cross section, which is unfavorable for wear performance. For the A356 alloy with the 1200 s precursor coating, the bi-layered structure has not been changed after the subsequent treatment in the electrolyte of 32 g/L $NaAlO_2$ + 10 g/L NaOH for 180 s, as shown in Fig. 8(d). The results presented here show that coatings with ideal dense single-layered structure have not been formed in the electrolyte with 10 g/L NaOH, no matter what kind of precursor coatings are employed.

3.6 Wear performances

The wear performances of the un-coated A356 alloy and the coatings formed in the concentrated aluminate electrolyte with the addition of different concentrations of NaOH have been evaluated by dry sliding tests against a WC ball. Figure 9(a) indicates the relationship between the friction coefficient and sliding time for the different samples. For the un-coated substrate of A356 alloy, the friction coefficient shows values of 0.7−0.74 from 0 to 35 s, after which it drops suddenly to about 0.5, and then the friction coefficient varies greatly between 0.46 and 0.64, reaching a final value of about 0.5 at 1800 s.

The behavior of the friction coefficient of the coatings is different from that of the uncoated substrate. As for the coating formed in 32 g/L $NaAlO_2$ + 1 g/L NaOH for 300 s, the friction coefficient gradually increases from a beginning value of about 0.4 to the maximum of 0.68 at 460 s, after which the coefficient begins to decline and suddenly drops to about 0.46 at 700 s, close to the value of the substrate in the friction experiment. It is believed that the coating is destroyed when the friction coefficient reduces rapidly (at about 700 s), which corresponds to the ‘transition point’ as reported by MARTINI et al [54]. After the transition point, the substrate is exposed to the WC ball so that the behavior of the friction coefficient is similar to that of the uncoated substrate. A similar situation occurs for the coating formed in 32 g/L

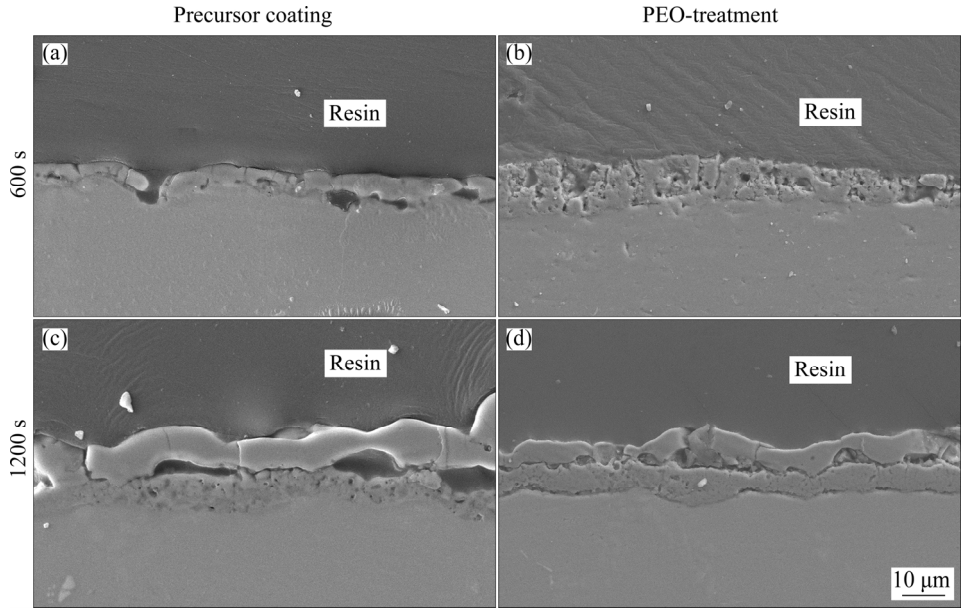

Fig. 8 Cross-sectional morphologies of precursor coating formed in 2 g/L $NaAlO_2$ +1 g/L NaOH for 600s (a) and 1200 s (c), and subsequent PEO-treatment in 32 g/L $NaAlO_2$ + 10 g/L NaOH for 180 s (b, d)

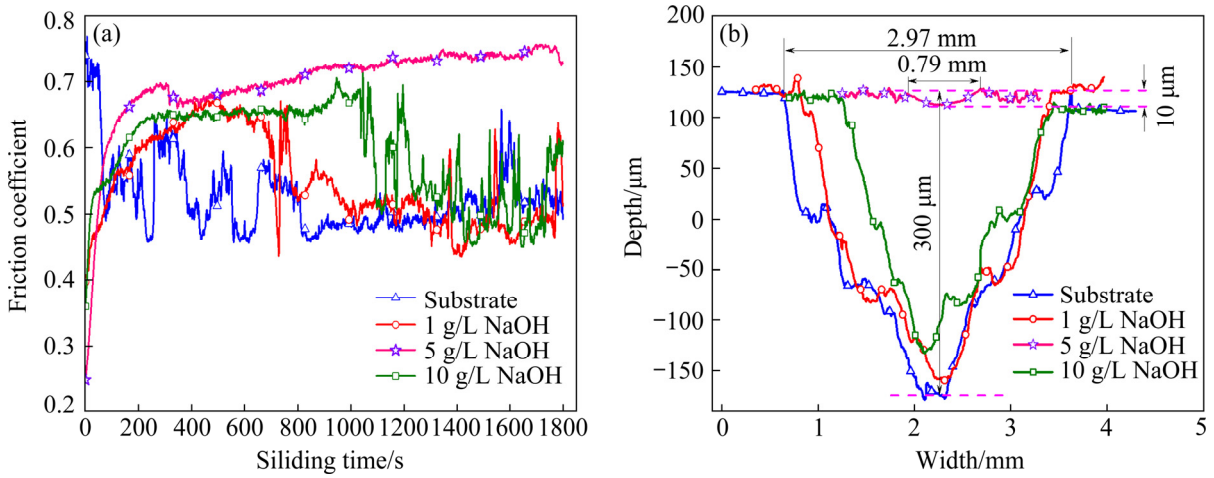

Fig. 9 Friction coefficient as function of sliding time (WC ball, 20 N load) for un-coated A356 alloy and coatings formed in 32 g/L $NaAlO_2$ electrolyte with addition of 1, 5 and 10 g/L NaOH (a) and corresponding wear scar profiles after dry sliding tests (b) (For the coatings formed with the addition of 1 and 5 g/L NaOH, 120 s precursor coating was employed and the treatment time was 300 s; For 10 g/L NaOH, the precursor coating was formed for 600 s and the treatment time in the concentrated aluminate was 180 s)

$NaAlO_2$ + 10 g/L NaOH for 180 s (600 s precursor coating was employed): a transition point appears at about 1034 s, and after that, large fluctuation in the coefficient is observed. However, no transition point has been observed for the dry sliding test of the coating fabricated in the electrolyte of 32 g/L $NaAlO_2$ + 5 g/L NaOH for 300 s. The coefficient of friction rises from about 0.25 to 0.70 in 294 s, after which the coefficient declines slightly and then rises again at very low rates to the final point of about 0.73 at 1800 s. The absence of a transition point indicates that the coating has not been damaged during the sliding test.

Figure 9(b) shows the wear scar profiles after dry sliding against WC ball for 1800 s under the load of 20 N for the coatings formed in 32 g/L $NaAlO_2$ electrolyte with the addition of 1, 5 and 10 g/L NaOH and the uncoated A356 substrate. It is shown that a minimum wear scar depth of about 10 μm is measured on the coating generated from the electrolyte of 32 g/L $NaAlO_2$ + 5 g/L NaOH, while the wear depth of the un-coated substrate is about 300 μm, and the depth on the other two coatings is close to that of the uncoated sample. As for the wear scar width, the coating produced in 32 g/L $NaAlO_2$ + 5 g/L NaOH gives rise to a value of 0.79 mm and that of the substrate is 2.97 mm. Based on wear scar profiles, the wear rate of each sample is further calculated and listed in Table 3. It can be seen that the wear rate for the substrate is as high as 2.94×10^{-5} $mm^3\cdot N^{-1}\cdot m^{-1}$, but the wear rate of the coating formed in the 32 g/L $NaAlO_2$ + 5 g/L NaOH electrolyte is only 4.1×10^{-7} $mm^3\cdot N^{-1}\cdot m^{-1}$. The wear rate of the coatings formed in 32 g/L $NaAlO_2$ with the addition of 1 and 10 g/L NaOH is close to that of the uncoated substrate. The high wear rates are because the substrate is no longer protected by the coatings after the transition point and the samples are seriously damaged by the WC ball under the high load of 20 N. The results show that the mechanical properties of A356 Al−Si alloy are low; while the un-destroyed coatings can effectively protect the alloy. Among all the coatings, the one developed in 32 g/L $NaAlO_2$ + 5 g/L NaOH electrolyte displays the best wear resistance because of its dense microstructure.

Figure 10 displays the SEM and three-

Table 3 Comparison of wear rates between coatings obtained from different electrolytes and un-coated substrate

Sample	Wear rate/ ($mm^3\cdot N^{-1}\cdot m^{-1}$)
Coatings obtained in 32 g/L $NaAlO_2$ + 1 g/L NaOH	2.59×10^{-5}
Coatings obtained in 32 g/L $NaAlO_2$ + 5 g/L NaOH	4.1×10^{-7}
Coatings obtained in 32 g/L $NaAlO_2$ + 10 g/L NaOH	1.67×10^{-5}
Substrate	2.94×10^{-5}

dimensional morphologies of wear scars on different samples after the friction tests. The results reveal that the substrate is seriously worn (Figs. 10(a, b)), followed by the coatings produced in 32 g/L $NaAlO_2$ electrolyte with the addition of 1 and 10 g/L NaOH (Figs. 10(c, d) and 10(g, h), respectively). In contrast, the coating produced in 32 g/L $NaAlO_2$ + 5 g/L NaOH electrolyte solution has not been worn through, showing the narrowest wear scar on the coating surface (Figs. 10(e, f)).

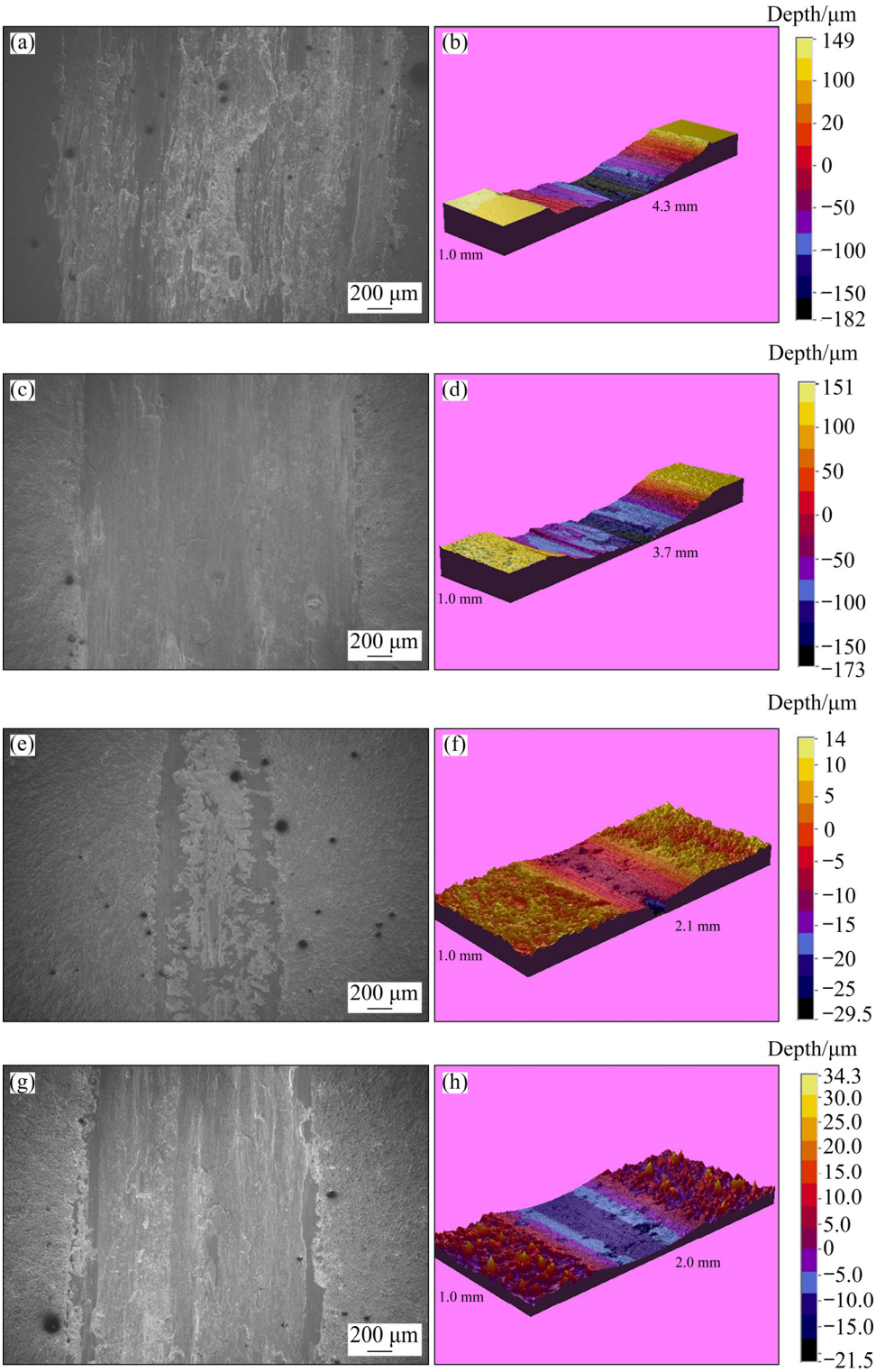

Fig. 10 Surface morphologies (a, c, e, g) and three-dimensional displays (b, d, f, h) of wear scars after dry sliding tests: (a, b) Un-coated substrate; (c, d) Coating formed in 32 g/L $NaAlO_2$ + 1 g/L NaOH electrolyte for 300 s (120 s precursor coating); (e, f) Coating formed in 32 g/L $NaAlO_2$ + 5 g/L NaOH electrolyte for 300 s (120 s precursor coating); (g, h) Coating formed in 32 g/L $NaAlO_2$ + 10 g/L NaOH electrolyte for 180 s (600 s precursor coating)

4 Discussion

Aluminate electrolytes have the advantage to form PEO coatings on Al alloys with the main components of alumina, which is a high-performance ceramic with promising properties. However, it was found that coatings obtained in low concentrated aluminate electrolytes have a double-layered structure, which is less wear-resistant when the load in the friction test is high [31]. Nevertheless, monolayer coatings with excellent wear performance can be prepared in a high concentration aluminate electrolyte (32 g/L $NaAlO_2$ + 1 g/L NaOH) [31]. However, the concentrated aluminate electrolyte is dis-advantageous for its poor stability which is unfavorable for industrial applications. It seems to be a contradiction that good electrolyte should provide high solubility for aluminate, but at the same time it must be aggressive to the Al substrate, oxide and oxo-hydroxides of aluminium. In this study, we demonstrate that the decomposition of aluminate electrolytes can be significantly suppressed by enhancing the concentration of NaOH in the electrolyte. The results show that the 32 g/L $NaAlO_2$ electrolyte with the addition of 1 g/L NaOH decomposes after 1 day of storage time, while the electrolyte can survive at least for 35 days with the addition of 5 g/L NaOH. As a result, improving the NaOH concentration would be a feasible way to enhance the stability of the aluminate electrolyte. However, the process of PEO of the alloy has been affected when more NaOH was added into the aluminate electrolyte. The precursor coating formed with a short time, e.g. 120 s, is not sufficient to guarantee the successful establishment of plasma discharges and the coating formation in the concentrated aluminate electrolyte. It is found that, when the NaOH concentration is increased to 10 g/L, longer pretreatment time of 10−1200 s in the dilute electrolyte is necessary for the subsequent PEO of the alloy in concentrated aluminate electrolyte. Notably, the long pretreatment time itself has some disadvantages, such as more energy consumption, and more importantly, the resultant coatings still are of poor quality, such as higher porosity and unaltered bi-layered feature. Hence, an optimum NaOH concentration should be selected, which can lead to longevity of aluminate electrolyte without sacrificing the quality of PEO coating. According to the results in this study, the addition of 5 g/L NaOH is the best choice, which can form coatings with excellent wear performance and only a precursor coating formed with short time (120 s) is required.

5 Conclusions

(1) The electrolyte of 32 g/L $NaAlO_2$ with the addition of 1 g/L NaOH decomposes after standing of about 24 h. In contrast, the addition of 5 g/L NaOH drastically improves the stability of the electrolyte up to about 35 days.

(2) The addition of NaOH affects the precursor coating required for the treatment in the concentrated aluminate electrolytes. For the PEO in the 32 g/L $NaAlO_2$ electrolytes with the addition of 1 and 5 g/L NaOH, a precursor coating formed for 120 s in the dilute electrolyte can be used. However, a precursor coating with a longer formation time of 600 s should be employed for the PEO treatment in 32 g/L $NaAlO_2$ + 10 g/L NaOH.

(3) The coating developed in the electrolyte of 32 g/L $NaAlO_2$ + 5 g/L NaOH is dense in micro-structure and displays the best wear resistance. The coatings formed in the electrolyte of 32 g/L $NaAlO_2$ + 10 g/L NaOH still show bi-layered structure like the coatings formed in dilute aluminate electrolyte or have greater porosity, and hence do not show good wear performance.

(4) The addition of 5 g/L NaOH to the concentrated aluminate electrolyte is an optimum choice, which not only improves the longevity of aluminate electrolyte but also leads to the formation of high-quality coatings.

Acknowledgments

The authors are grateful for the financial support from the National Natural Science Foundation of China (No. 51671084).

References

[1] AUIRRE-DE LA TORRE E, AFELTRA U, GOMEZ-ESPARZA C D, CAMARILLO-CISNEROS J, PEREZ-BUSTAMANTE R, MARTINZ-SANCHEZ R. Grain refiner effect on the microstructure and mechanical properties of the A356 automotive wheels [J]. Journal of Materials Engineering and Performance, 2014, 23(2): 581− 587.

[2] COLE G S, SHERMAN A M. Light weight materials for

automotive applications [J]. Materials Characterization, 1995, 35(1): 3−9.

[3] XU Fang-tao, XIA Yuan, LI Guang. The mechanism of PEO process on Al−Si alloys with the bulk primary silicon [J]. Applied Surface Science, 2009, 255(23): 9531−9538.

[4] GULEC A E, GENCER Y, TARAKCI M. The characterization of oxide based ceramic coating synthesized on Al−Si binary alloys by microarc oxidation [J]. Surface & Coatings Technology, 2015, 269(15): 100−107.

[5] SHAH K B, KUMAR S, DWIVEDI D K. Aging temperature and abrasive wear behaviour of cast Al−(4%, 12%, 20%)Si−0.3%Mg alloys [J]. Materials & Design, 2007, 28(6): 1968−1974.

[6] NOGITA K, YASUDA H, YOSHIDA K, UESUGI K, TAKEUCHI A, SUZUKI Y, DAHLE A K. Determination of strontium segregation in modified hypoeutectic Al−Si alloy by micro X-ray fluorescence analysis [J]. Scripta Materialia, 2006, 55(9): 787−790.

[7] SU Jun-feng, NIE Xue-yuan, HU H, TJONG J. Friction and counterface wear influenced by surface profiles of plasma electrolytic oxidation coatings on an aluminium A356 alloy [J]. Journal of Vacuum Science & Technology A, 2012, 30(6): 061402.

[8] XUE Wen-bin, SHI Xiu-ling, HUA Ming, LI Yong-liang. Preparation of anti-corrosion films by microarc oxidation on an Al−Si alloy [J]. Applied Surface Science, 2007, 253(14): 6118−6124.

[9] REZAEI M, JESHVAGHANI R A, SHAHVERDI H R, MOJAVER R, TORKAMANY M J. Formation of Ni-rich aluminide layers on an A356 aluminum alloy by a combined electroplating/laser alloying treatment: Microstructure and tribological characteristics [J]. Journal of Manufacturing Processes, 2017, 29: 310−319.

[10] ABEDINI B, PARVINI AHMADI N, YAZDANI S, MAGAGNIN L. Electrodeposition and corrosion behavior of An−Ni−Mn alloy coatings deposited from alkaline solution [J]. Transactions of Nonferrous Metals Society of China, 2020, 30(2): 548−558.

[11] CHRISTOGLOU C, VOUDOURIS N, ANGELOPOULOS G N, PANT M, DAHL W. Deposition of aluminium on magnesium by a CVD process [J]. Surface & Coatings Technology, 2004, 184(2−3): 149−155.

[12] ALTUN H, SEN S. The effect of PVD coatings on the corrosion behaviour of AZ91 magnesium alloy [J]. Materials & Design, 2006, 27(10): 1174−1179.

[13] ZHOU Qin-yi, TIAN Meng-meng, YING Zong-rong, DAN Yu-xin, TANG Feng-rui, ZHANG Jian-peng, ZHU Jun-wu, ZHU Xu-fei. Dense films formed during Ti anodization in NH4F electrolyte: Evidence against the field-assisted dissolution reaction of fluoride ions [J]. Electrochemistry Communications, 2020, 111: 106663.

[14] DAROONPARVAR M, MAT YAJID M A, KUMAR GUPTA R, MOHD YUSOF N, BAKHSHESHI-RAD H R, GHANDVAR H, GHASEMI E. Antibacterial activities and corrosion behavior of novel PEO/nanostructured ZrO_2 coating on Mg alloy [J]. Transactions of Nonferrous Metals Society of China, 2018, 27(8): 1571−1581.

[15] WANG Zhi-hu, ZHANG Ju-mei, LI Yan, BAI Li-jiang, ZHANG Guo-jun. Enhanced corrosion resistance of micro-arc oxidation coated magnesium alloy by superhydrophobic Mg−Al layered double hydroxide coating [J]. Transactions of Nonferrous Metals Society of China, 2019, 29(10): 2066−2077.

[16] AN Ling-yun, MA Ying, YAN Xiao-xu, WANG Sheng, WANG Zhan-ying. Effects of electrical parameters and their interactions on plasma electrolytic oxidation coatings on aluminum substrates [J]. Transactions of Nonferrous Metals Society of China, 2020, 30(4): 883−895.

[17] ZHU Yuan-yuan, GAO Wei-dong, HUANG Hua-de, CANG Wen-hui, ZHANG Shu-fang, ZHANG Rong-fa, ZHAO Rong-fang, ZHANG Yi-jia. Investigation of corrosion resistance and formation mechanism of calcium-containing coatings on AZ31B magnesium alloy [J]. Applied Surface Science, 2019, 487(1): 581−592.

[18] XIE Huan-jun, CHENG Ying-liang, LI Shao-xian, CAO Jin-hui, CAO Li. Wear and corrosion resistant coatings on surface of cast A356 aluminum alloy by plasma electrolytic oxidation in moderately concentrated aluminate electrolytes [J]. Transactions of Nonferrous Metals Society of China, 2017, 27(2): 336−351.

[19] ZHANG Rong-fa. Film formation in the second step of micro-are oxidation on magnesium alloys [J]. Corrosion Science, 2010, 52(4): 1285−1290.

[20] LIANG J, BALA SRINIVASAN P, BLAWERT C, STORMER M, DIETZEL W. Electrochemical corrosion behaviour of plasma electrolytic oxidation coatings on AM50 magnesium alloy formed in silicate and phosphate based electrolytes [J]. Electrochimica Acta, 2009, 54(14): 3842−3850.

[21] WANG Shu-qi, WANG Ya-ming, CUI Yi, ZOU Yong-chun, WU Yun-feng, CHEN Guo-liang, JIA De-chang, ZHOU Yu. High voltage resistance ceramic coating fabricated on titanium alloy for insulation shielding application [J]. Ceramics International, 2019, 45(2): 1909−1917.

[22] LI Guo-qiang, WANG Ya-ping, QIAO Li-ping, ZHAO Rong-fang, ZHANG Shu-fang, ZHANG Rong-fa, CHEN Chun-mei, LI Xin-yi, ZHAO Ying. Preparation and formation mechanism of copper incorporated micro-arc oxidation coatings developed on Ti−6Al−4V alloys [J]. Surface & Coatings Technology, 2019, 375(15): 74− 85.

[23] CHENG Ying-liang, WANG Ting, Li Shao-xian, CHENG Yu-lin, CAO Jun-hui, XUE Huan-jun. The effects of anion deposition and negative pulse on the behaviours of plasma electrolytic oxidation (PEO)−Asystematic study of the PEO of a Zirlo alloy in aluminate electrolytes [J]. Electrochimica Acta, 2017, 225(20): 47−68.

[24] WEI Ke-jian, ZHANG Yi-fan, YU Jia-hao, LIU Rui-hong, DU Jian-cheng, JIANG Fu-bin, XUE Wen-bin. Analyses of hydrogen release on Zirlo alloy anode during plasma electrolytic oxidation [J]. Materials Chemistry and Physics, 2020, 251(1): 123054.

[25] CHENG Ying-liang, CAO Jin-hui, MAO Mo-ke, XIE Huan-jun, SKELDON P. Key factors determining the development of two morphologies of plasma electrolytic coatings on an Al−Cu−Li alloy in aluminate electrolytes [J]. Surface & Coatings Technology, 2016, 291(15): 239−249.

[26] SNIZHKO L O, YEROKHIN A L, PILKINGTON A, GUREVINA N L, MISNYANKIN D O, LAYLAND A,

MATTHEWS A. Anodic processes in plasma electrolytic oxidation of aluminium in alkaline solutions [J]. Electrochimica Acta, 2004, 49(13): 2085−2095.

[27] CHENG Ying-liang, MAO Mo-ke, CAO Jin-hui, PENG Zhao-mei. Plasma electrolytic oxidation of an Al−Cu−Li alloy in alkaline aluminate electrolytes: A competition between growth and dissolution for the initial ultra-thin films [J]. Electrochimica Acta, 2014, 138(20): 417−429.

[28] YEROKHIN A L, NIE X Y, LEYLAND A, MATTHEWS A, DOWEY S J. Plasma electrolysis for surface engineering [J]. Surface & Coatings Technology, 1999, 122(2−3): 73−93.

[29] HAN Jun-xiang, CHENG Yu-lin, TU Wen-bin, ZHAN Ting-yan, CHENG Ying-liang. The black and white coatings on Ti−6Al−4V alloy or pure titanium by plasma electrolytic oxidation in concentrated silicate electrolyte [J]. Applied Surface Science, 2018, 428(15): 684−697.

[30] TSENG C C, LEE J L, KUO T H, KUO S N, TSENG K H. The influence of sodium tungstate concentration and anodizing conditions on microarc oxidation (MAO) coatings for aluminum alloy [J]. Surface & Coatings Technology, 2012, 206(16): 3437−3443.

[31] CHENG Ying-liang, CAO Jin-hui, MAO Mo-ke, PENG Zhao-mei, SKELDON P, THOMPSON G E. High growth rate, wear resistant coatings on an Al−Cu−Li alloy by plasma electrolytic oxidation in concentrated aluminate electrolytes [J]. Surface & Coatings Technology, 2015, 269(15): 74−82.

[32] PAN Xiao-lin, YU Hai-yan, TU Gan-feng, BI Shi-wen. Effects of precipitation activity of desilication products (DSPs) on stability of sodium aluminate solution [J]. Hydrometallurgy, 2016, 165(2): 261−269.

[33] MOON S, JEONG Y. Generation mechanism of microdischarges during plasma electrolytic oxidation of Al in aqueous solutions [J]. Corrosion Science, 2009, 51(7): 1506−1512.

[34] CHENG Ying-liang, XUE Zhi-gang, WANG Qun, WU Xiang-quan, MATYKINA E, SKELDON P, THOMPSON G E. New findings on properties of plasma electrolytic oxidation coatings from study of an Al−Cu−Li alloy [J]. Electrochimica Acta, 2013, 107(30): 358−378.

[35] MALSTEV G Z, MALININ G V, MASHOVETS V P. The structure of aluminate solutions [J]. Journal of Structural Chemistry, 1966, 6(3): 359−362.

[36] CARREIRA L A, MARONI V A. Raman and infrared spectra and structures of the aluminate ions [J]. The Journal of Chemical Physics, 1966, 45(6): 2216−2220.

[37] MOOLENAAR R J, EVANS J C, MCKEEVER L D. Structure of the aluminate ion in solutions at high pH [J]. The Journal of Physical Chemistry, 1970, 74(20): 3629−3636.

[38] SWEEGERS C, MEEKES H, van ENCKEVORT W J P, HIRALAL I D K, RIJKEBOER A. Growth rate analysis of gibbsite single crystals growing from aqueous sodium aluminate solutions [J]. Crystal Growth & Design, 2004, 4(1): 185−198.

[39] LIU Gui-hua, LI Zheng, QI Tian-gui, ZHOU Qiu-sheng, PENG Zhi-hong, LI Xiao-bin. Continuous changes in electrical conductivity of sodium aluminate solution in seeded precipitation [J]. Transactions of Nonferrous Metals Society of China, 2015, 25(12): 4160−4166.

[40] EREMIN N I, VOLOKHOV Y A, MIRONOV V E. Structure and behavior of aluminate ions in solution [J]. Russian Chemical Reviews, 1974, 43(2): 92−106.

[41] CHEN Nian-yi, LIU Miao-xiu, CAO Yi-lin, TANG Bo, HONG Mei. Studies on the anionic species of sodium aluminate solutions [J]. Science in China Series B−Chemistry, Life Sciences & Earth Sciences, 1993, 36(1): 32−38. (in Chinese)

[42] DUAN Jian-guo, DONG Peng, WANG Ding, LI Xue, XIAO Zheng-wei, ZHANG Ying-jie, HU Guo-rong. A facile structure design of $LiNi_{0.90}Co_{0.07}Al_{0.03}O_2$ as advanced cathode materials for lithium ion batteries via carbonation decomposition of $NaAl(OH)_4$ solution [J]. Journal of Alloys and Compounds, 2018, 739(30): 335−344.

[43] CHEN Nian-yi. Physical chemistry of alumina production [M]. Shanghai: Shanghai Science and Technology Press, 1962. (in Chinese)

[44] LI Yan, ZHANG Yi-fei, YANG Chao, ZHANG Yi. Precipitating sandy aluminium hydroxide from sodium aluminate solution by the neutralization of sodium bicarbonate [J]. Hydrometallurgy, 2009, 98(1−2): 52−57.

[45] SATO T, SATO S, OKUWAKI A. The improvement in the corrosion resistance of alumina in caustic alkaline solutions obtained by dispersing ceria-doped tetragonal zirconia particles [J]. Corrosion Science, 1992, 33(4): 581−585.

[46] DOCHE M L, RAMEAU J J, DURAND R, NOVEL-CATTIN F. Electrochemical behaviour of aluminium in concentrated NaOH solutions [J]. Corrosion Science, 1999, 41(4): 805−826.

[47] O'SULLIVAN J P, WOOD G C. The morphology and mechanism of formation of porous anodic films on aluminium [J]. Proceedings of the Royal Society of London. Series A: Mathematical and Physical Sciences, 1970, 317: 511−543.

[48] MONFORT F, BERKANI A, MATYKINA E, SKELDON P, THOMPSON G E, HABAZAKI H, SHIMIZU K. Development of anodic coatings on aluminium under sparking conditions in silicate electrolyte [J]. Corrosion Science, 2007, 49(2): 672−693.

[49] LV Guo-hua, GU Wei-chao, CHEN Huan, FENG Wen-ran, LATIF KHOSA M, LI Li, NIU Erwu, ZHANG Gu-ling, YANG Si-ze. Characteristic of ceramic coatings on aluminum by plasma electrolytic oxidation in silicate and phosphate electrolyte [J]. Applied Surface Science, 2006, 253(5): 2947−2952.

[50] LEE K M, KO Y G, SHIN D H. Incorporation of multi-walled carbon nanotubes into the oxide layer on a 7075 Al alloy coated by plasma electrolytic oxidation: Coating structure and corrosion properties [J]. Current Applied Physics, 2011, 11(4): s55−s59.

[51] DEHNAVI V, LUAN B L, SHOESMITH D W, LIU Xing-yang, ROHANI S. Effect of duty cycle and applied current frequency on plasma electrolytic oxidation (PEO) coating growth behavior [J]. Surface & Coatings Technology, 2013, 226(15): 100−107.

[52] IKONOPISOV S. Theory of electrical breakdown during formation of barrier anodic films [J]. Electrochimica Acta, 1977, 22(10): 1077−1082.

[53] YANG Zhong, ZHANG Xu-zhen, WU Ye-kang, WANG Dong-dong, LIU Xin-tong, WU Guo-rui, NASH P, SHEN De-jiu. Plasma electrolytic oxidation ceramic coatings proceed by porous anodic film [J]. Journal of Alloys and Compounds, 2020, 812(5): 152098.

[54] MARTINI C, CESCHINI L, TARTERINI F, PAILLARD J M, CURRAN J A. PEO layers obtained from mixed aluminate-phosphate baths on Ti−6Al−4V: Dry sliding behaviour and influence of a PTFE topcoat [J]. Wear, 2010, 269(11−12): 747−756.

氢氧化钠对中等浓度铝酸盐电解液中 A356 铝合金等离子体电解氧化的影响

程昱琳[1]，谢焕钧[2]，曹金晖[3]，程英亮[1]

1．湖南大学 材料科学与工程学院，长沙 410082；
2．中国航发中传机械有限公司，长沙 410200；
3．湖南大学 化学与化工学院，长沙 410082

摘　要：在 32 g/L 铝酸钠中加入不同浓度的氢氧化钠，对铸造 A356 铝合金进行等离子体电解氧化(PEO)处理。通过增加 NaOH 的浓度，铝酸盐溶液的稳定性大大提高。然而，由于氢氧化钠浓度的增加，PEO 的行为发生相应的变化。在更高浓度的氢氧化钠电解液中，对 A356 铝合金进行 PEO 处理时需要较厚的预生膜。结果表明，NaOH 的最佳浓度为 5 g/L，可将贮存电解液的稳定性提高至 35 天，并能获得高耐磨致密陶瓷膜层(磨损率为 $4.1\times10^{-7}mm^3\cdot N^{-1}\cdot m^{-1}$)。

关键词：等离子体电解氧化；耐磨性；铝酸钠；氢氧化钠；A356 合金

(Edited by Bing YANG)